Solar Energy
And Sustainable Development
Refereed, biannual scientific journal issued by:
The Libyan Center for Solar Energy Research and Studies

Power Management in a PV-Battery Microgrid Using Hybrid ANFIS-Fuzzy Logic MPPT Control and an Adaptive Charge-Discharge Algorithm

Mohamed Amine Atillah[1*], Hicham Stitou[2], Abdelghani Boudaoud[3], Mounaim Aqil[4].

[1,2,3,4]Engineering and Applied Physics Team (EAPT), Superior School of Technology, Sultan Moulay Slimane University, Beni Mellal, Morocco.

E-*mail:* [1] mohamedamine.atillah@usms.ma.

ARTICAL INFO:

The 1St International Conference on Sciences and Techniques for Renewable Energy and the Environment.
(STR2E 2025)
May 6-8, 2025 at FST-Al Hoceima-Morocco.

KEYWORDS

PV; Battery; Microgrid; ANFIS; Fuzzy logic; MPPT; Partial shading.

ABSTRACT

This work presents an energy management strategy (EMS) for a microgrid that integrates photovoltaic (PV) panels, a battery energy storage system (BESS), and a grid connection. The primary objective is to maintain a dynamic and reliable power balance between PV generation, local load, BESS, and the grid, while maximizing the self-consumption of solar energy. The system architecture comprises a PV generator whose power is optimized by a hybrid Maximum Power Point Tracking (MPPT) algorithm that integrates an Adaptive Neuro-Fuzzy Inference System (ANFIS) and a fuzzy controller, acting as a PI regulator.

The BESS, made up of Lithium-ion batteries, is managed by a bi-directional DC-DC converter and a fuzzy PI controller, which ensures fine, adaptive regulation of power flows. The core of the innovation lies in the battery management algorithm, which relies on a set of explicit rules to direct power flows. These rules include a strict 10 kW constraint on battery charging and discharging power, crucial for preserving battery life and system safety. The system was simulated considering various cases of irradiance profiles and charging demands of 35 kW and 55 kW, including normal and critical battery state-of-charge (SOC) situations. The simulation results demonstrate the success of the ANFIS-Fuzzy Logic (FL) MPPT control in maximizing energy capture with an error of ± 0.06 KW, while the BESS keeps power balance error below ± 0.02 kW in all tested scenarios. These results confirm the algorithm's ability to handle critical high and low SOC situations, intelligently redirecting power flows to maintain microgrid stability and power continuity.

*Corresponding author.

DOI: https://doi.org/10.51646/jsesd.v14i2.1198

إدارة الطاقة في شبكة كهربائية تعمل بالطاقة الشمسية والبطاريات باستخدام نظام تحكم هجين باستخدام النظام العصبي الضبابي التكيفي والمنطق الضبابي لتتبع نقطة الطاقة القصوى وخوارزمية شحن وتفريغ قابلة للتكيف

عاطي اللّه محمد أمين، وستيتوهشام، وبوداود عبد الغاني، وعاقل منعيم.

ملخص: يقدم هذا العمل استراتيجية لإدارة الطاقة لشبكة كهربائية تدمج الألواح الكهروضوئية ونظام تخزين الطاقة بالبطاريات ووصلة الشبكة. الهدف الأساسي هو الحفاظ على توازن ديناميكي وموثوق بين توليد الطاقة الكهروضوئية والحمل المحلي ونظام تخزين الطاقة بالبطاريات والشبكة، مع تعظيم الاستهلاك الذاتي للطاقة الشمسية. تتكون بنية النظام من مولد كهروضوئي يتم تحسين طاقته بواسطة خوارزمية هجينة لتتبع نقطة الطاقة القصوى تدمج نظام الاستدلال العصبي الضبابي التكيفي ووحدة تحكم ضبابية تعمل كمنظم. يتم إدارة نظام تخزين الطاقة بالبطاريات، المكون من بطاريات ليثيوم أيون، بواسطة محول تيار مستمر ثنائي الاتجاه ووحدة تحكم ضبابية، مما يضمن تنظيمًا دقيقًا وتكيفيًا لتدفقات الطاقة. يكمن جوهر الابتكار في خوارزمية إدارة البطارية، التي تعتمد على مجموعة من القواعد الصريحة لتوجيه تدفقات الطاقة. تتضمن هذه القواعد قيودًا صارمة تبلغ 10 كيلوواط على شحن البطارية وتفريغها، وهو أمر بالغ الأهمية للحفاظ على عمر البطارية وسلامة النظام. تمت محاكاة النظام مع الأخذ في الاعتبار حالات مختلفة من ملامح الإشعاع ومتطلبات الشحن التي تبلغ 35 كيلوواط و 55 كيلوواط، بما في ذلك حالات الشحن العادية والحرجة للبطارية. تظهر نتائج المحاكاة نجاح التحكم في تعظيم التقاط الطاقة بخطأ ± 0.06 كيلوواط، بينما يحافظ على خطأ توازن الطاقة أقل من ± 0.02 كيلوواط في جميع السيناريوهات التي تم اختبارها. تؤكد هذه النتائج قدرة الخوارزمية على التعامل مع الحالات الحرجة لارتفاع وانخفاض حالة شحن البطارية، وإعادة توجيه تدفقات الطاقة بذكاء للحفاظ على استقرار الشبكة الصغيرة واستمرارية الطاقة.

الكلمات المفتاحية: الطاقة الكهروضوئية، بطاريات، شبكة كهربائية، النظام العصبي الضبابي التكيفي، المنطق الضبابي، تتبع نقطة الطاقة القصوى، التظليل الجزئي..

1. INTRODUCTION

The global energy transition to renewable energy sources is imperative for mitigating climate change and ensuring sustainable development. In this context, microgrids are emerging as a key solution to facilitate the massive integration of renewable energies, particularly photovoltaic energy [1]. Microgrids offer multiple benefits, such as improved reliability and efficiency of energy supply, greater resilience to main grid failures, and the ability to operate autonomously or connected to the power grid [2][3]. Solar photovoltaic energy, in particular, is growing exponentially due to its lower costs and environmentally friendly nature. However, PV production is highly intermittent and variable, depending as it does on weather conditions (Irradiation, temperature), which poses significant challenges to the stability and management of power grids [4]. To compensate for this intermittency and ensure a stable, reliable energy supply, battery energy storage systems (BESS) are becoming increasingly important. BESS allows excess PV energy produced during periods of high sunshine to be stored for later use when PV production is low or non-existent, or when load demand is high [5]. This ability to temporally decouple production and consumption is essential for maximizing self-consumption of PV energy, reducing dependence on the grid, and improving overall microgrid performance. Efficient power management within a PV-battery-grid system is therefore of primary importance.

The power output of a photovoltaic panel is not constant; it varies considerably according to the ambient conditions, such as solar irradiance and temperature [6]. To optimize the efficiency of

PV systems and maximize the electrical power generated, it is essential to permanently extract the maximum power point (MPP) available [7][8]. Without MPPT, a PV system would often operate below its optimum potential, resulting in a significant loss of energy and a reduction in overall efficiency.

In the field of microgrid power management, several recent works have explored various facets. Previous research has investigated hybrid MPPT under various operating conditions. The novelty of this work lies in the use of ANFIS, a relatively innovative technique, combined with a fuzzy logic–based controller to enhance performance and adaptability. For example, Siddaraj et al [9] have proposed a hybrid MPPT method based on Particle Swarm Optimization (PSO) and ANFIS to improve power generation and conversion in a microgrid, while maintaining voltage and frequency stability. However, the management of extreme cases of battery charge and discharge is not addressed. From a flexibility perspective, Kalaiyarasan et al [10] in another study developed an energy management system for a DC microgrid integrating PV sources and fuel cells, using ANFIS controllers for MPPT and bidirectional converters for battery charge/discharge control. But source prioritization (PV - battery - grid priority) and real-time power surplus/deficit management are not detailed. Other researchers, such as Dhanunjaya et al [11], have focused on an ANFIS controller-based energy management system for a smart DC microgrid, combining PV, wind sources, and a battery bank, to improve power quality and power extraction efficiency. The study focuses on isolated DC microgrids without interaction with an external grid, and transitions between modes (critical charge/discharge) are not addressed.

However, despite these advances, there is still a lack of integrated approaches that combine high-performance MPPT control with an adaptive battery management algorithm capable of handling both normal and critical State of Charge (SOC) conditions in grid-connected PV-battery microgrids. In particular, existing studies often overlook strict power constraints for battery protection (e.g., maximum charge/discharge limits) and real-time prioritization of energy flows between PV, battery, and grid. This gap limits the applicability of these systems in scenarios requiring both high efficiency and operational safety.

Faced with this state-of-the-art, our work distinguishes itself by implementing an MPPT control based on an ANFIS, a method recognized for its high efficiency and rapid response to variations in sunlight conditions. In addition, a fuzzy logic controller is used for fine-tuning, acting as an enhanced PI controller. The specificity of our contribution also lies in the battery management algorithm, which strictly integrates a charge/discharge power limit of 10 kW and defines a precise system behaviour when the battery reaches its extreme states of charge (fully charged or discharged). The aim is to ensure efficient and reliable power balancing between photovoltaic generation, load, battery, and grid while respecting essential practical constraints.

The organization of this article is as follows: Section 2 is dedicated to the methodologies and materials used, Section 3 analyzes the results obtained, and Section 4 presents the conclusion and future scope.

2. Methodology and Materials

The architecture of the microgrid studied is illustrated in Fig.1, showing the interconnection of various components. The system includes a photovoltaic generator, a DC- DC boost converter equipped with an MPPT algorithm, a BESS with its bidirectional DC-DC converter , a DC-AC inverter with control to regulate voltage, an AC load, and the electrical grid.

The study presented in this article will focus on maximizing the power extracted from PV panels, whatever the irradiation conditions (uniform or partial), and on balancing the power flows between PV, battery, and grid, based on the battery charge/discharge management algorithm.

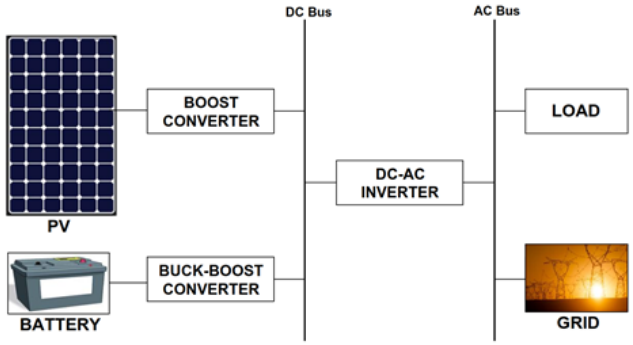

Fig.1. PV-Battery Microgrid architecture.

2.1. PV Generator specifications

The PV generator is made up of 3 three photovoltaic panels (as presented in Fig.2) with a total peak power of 50KW for a solar irradiation of 1000 W/m² and a temperature of 25°C.

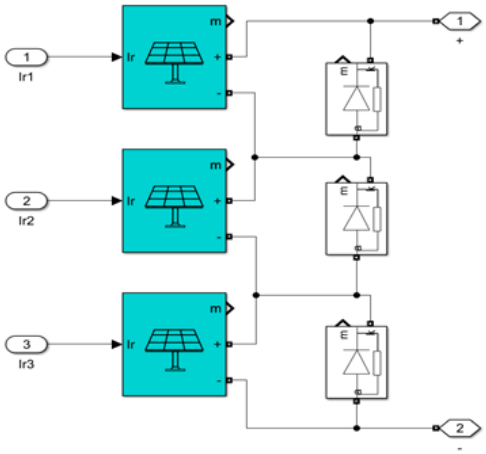

Fig.2. The PV generator used.

To study and analyze photovoltaic system performance, it's essential to distinguish between two main sunlight conditions: uniform irradiation and partial shading. Uniform irradiation represents a situation where all panels receive the same level of irradiation. Partial shading, on the other hand, occurs when different parts of the PV field are exposed to varying levels of irradiance, which is a realistic scenario due to obstacles such as clouds, buildings, or trees [12].

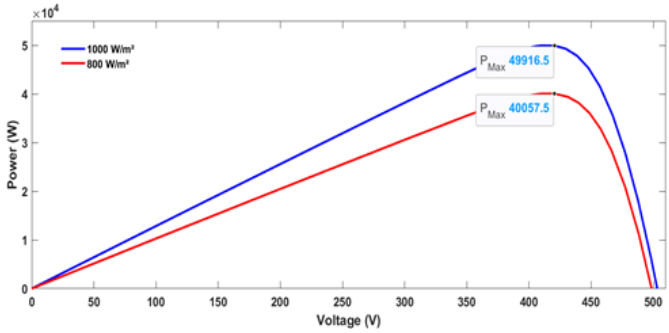

Fig.3. Electrical characteristics under uniform irradiance.

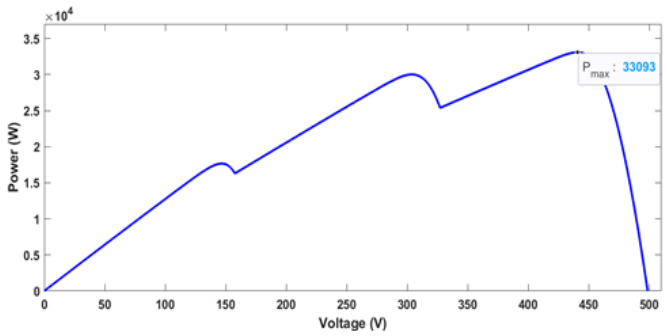

Fig.4. Electrical characteristics under partial shading.

To simulate uniform irradiance, two levels were applied simultaneously to all the panels in the array: first 1000 W/m², then 800 W/m² to represent a drop in irradiance. For partial shading, each group of panels received a separate irradiance: 1000 W/m² for the first, 800 W/m² for the second, and 600 W/m² for the third, thus reproducing a non-uniform distribution of irradiance. The panel characteristics are presented in Fig.3 and Fig.4.

2.1.1. ANFIS–FL MPPT

Our MPPT control system is designed around three main blocks, working together to optimize photovoltaic production as presented in Fig.5.

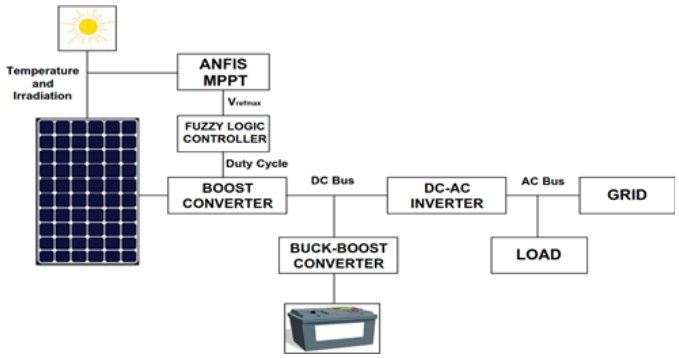

Fig.5. ANFIS-FL MPPT principle.

The first block is an ANFIS. Specifically trained to predict the voltage at the point of maximum power (VMPP) as a function of solar irradiation and ambient temperature. In this study, the focus is on irradiance variation, with temperature considered a constant parameter.
The second block is a fuzzy logic (FL) controller. This controller acts as a PI-type regulator whose function is to keep the output voltage of the photovoltaic panel equal to the reference VMPP determined by the ANFIS. It receives this reference VMPP as input and generates the duty cycle for the DC-DC Boost converter [13]. The choice of an FL controller is justified by the non-linear nature of the small-signal model of a PV system coupled to a boost converter. Unlike conventional controllers, which require a precise mathematical model, the FL controller relies on heuristic knowledge and general rules of the system, enabling it to operate efficiently in this non-linear environment. Finally, the third block is the DC-DC Boost converter. Placed between the photovoltaic panel and the DC-AC inverter, this converter (illustrated in Fig.6) is controlled by the duty cycle provided by the FL controller. Its purpose is to adjust the impedance seen by the PV panel to ensure that the system operates constantly at the point of maximum power [12].

2.1.2. ANFIS model

The ANFIS is a hybrid technique that combines the adaptive learning capabilities of neural networks with FL [14] [15], offering a powerful approach to energy management and MPPT

in PV systems. The ANFIS architecture consists of five distinct layers: the fuzzification layer, the rules layer, the normalization layer, the consequent layer, and the addition layer. The ANFIS architecture is detailed in [16].

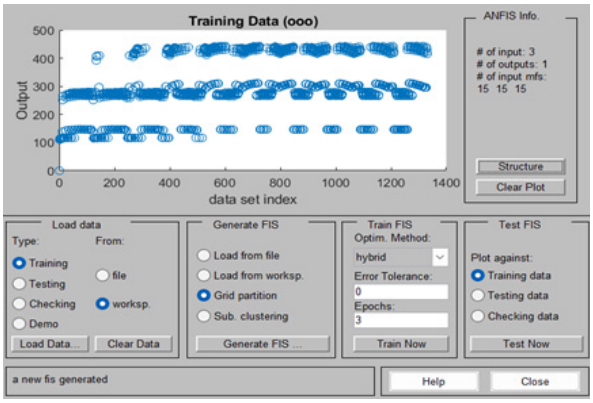

Fig.6. Configuration interface of the ANFIS designer in MATLAB.

The ANFIS model is designed using the neuro-fuzzy design tool available in the MATLAB environment, illustrated in Fig.6.

To design the ANFIS model, 1400 training data are used (Table 1 shows a selection of these data); this data is derived from MATLAB/Simulink simulations of the proposed microgrid system. On the input side, the data correspond to the irradiances of the three PV panels, while on the output side, the model provides the voltage corresponding to the point of maximum power. The type of membership function is triangular, with 15 membership functions for the three inputs and 3 epochs. The designer then performs training on the ANFIS model, adaptively adjusting the system parameters to achieve optimum accuracy [17]. The results are encouraging, with a root- mean-square error (RMSE) of around 8.6×10-4.

Table 1. Selection of training data.

Irradiation Pv1	Irradiation Pv2	Irradiation Pv3	Voltage of MPP
1000	1000	1000	415.49
800	600	100	304.90
800	100	100	146.76
100	800	100	146.76
300	600	500	271.92
400	700	1000	274.70
900	400	600	441.89
600	300	400	435.41
400	800	900	269.30
200	800	800	266.48

2.1.3. FL controller

The FL controller design method, Rules for error and error variation, and the membership functions for the input and output variables are detailed in [18][19][20]. The interpretation used for the rules is Mandani, and the Defuzzification used is Centroid.

On completion of the design, the controller is implemented in Simulink, as shown in Fig.7.

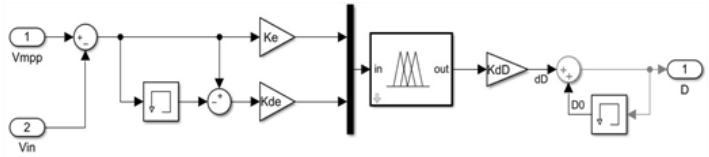

Fig.7. Implementation of FL controller in MATLAB/Simulink.

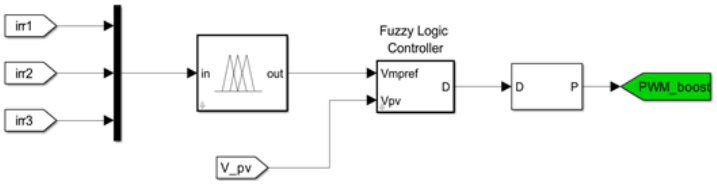

Fig.8. Complete Simulink implementation of the hybrid ANFIS–Fuzzy Logic MPPT controller.

In order to implement the control, MATLAB Simulink was used, based on the system components presented above. The simulation of the MPPT controller is illustrated in Fig.8.

2.1.4. DC-DC Boost Converter

The DC-DC boost converter, presented in Fig.9, is an essential component in the photovoltaic chain, with two crucial roles. Firstly, it increases the output voltage of the photovoltaic panels to a desired level, avoiding the need to increase the number of panels connected in series to achieve a higher voltage [13]. Secondly, and just as importantly, it controls the operating point of the PV-load assembly. By adjusting its duty cycle, this converter enables the system to constantly monitor the panels' MPP [21].

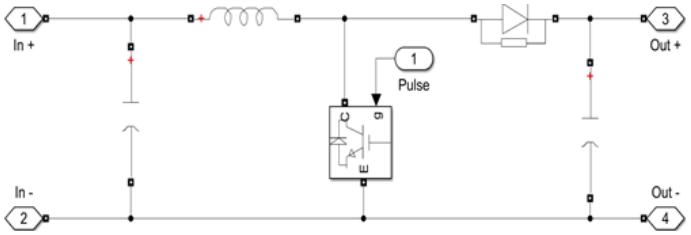

Fig.9. Schematic of the DC–DC boost converter.

The boost output voltage is related to the input voltage by the relationship below [12].

$$V_o = \frac{\text{Vi}}{1 - \text{D}} \qquad (1)$$

Where: D: Duty cycle. Vi: Input voltage. V_o : Output voltage ripple.

2.2. Battery energy storage systems

2.2.1. BESS Components and Specifications

The BESS is an essential pillar of the microgrid, playing a crucial role in the dynamic balancing of intermittent PV panel production and fluctuating load demand. Its importance lies in its ability to store excess solar energy for later use, and to make up power deficits when PV production is insufficient.

The BESS uses a lithium-ion battery with a capacity of 150 Ah. A fundamental operational constraint is the limitation of its charging and discharging power to a maximum of 10 kW. These specifications are used exclusively to check the algorithm's performance and are not based on any particular dimensioning. The battery block in Simulink is shown in Fig.10.

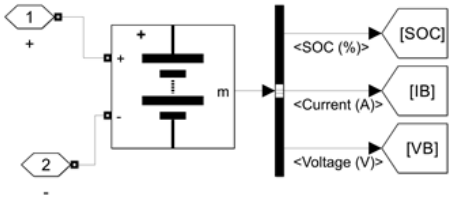

Fig.10. Battery block in Simulink.

Connecting and controlling the battery to the microgrid's DC bus is a bidirectional DC-DC converter (presented in Fig.11), essential for managing power flows in both directions (charge and discharge). This converter is regulated by a control loop, typically a PI controller, which adjusts the battery current according to system requirements to maintain energy balance [23].

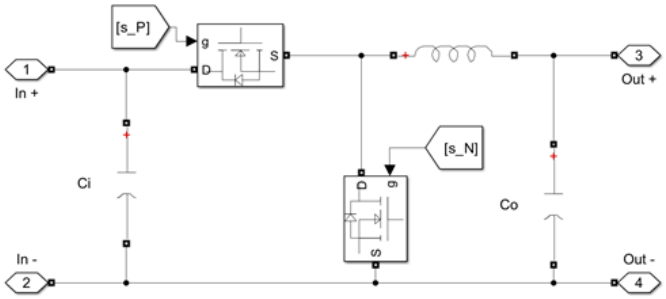

Fig.11. Schematic of the Bi-directional buck-boost converter.

2.2.2. Rule-Based Intelligence in Critical SOC Handling

The battery management strategy is based on maintaining the battery's SOC between safe thresholds of 20% (SOCmin) and 80% (SOCmax), to preserve battery life and ensure system safety [21]. The energy management algorithm is the brain behind this coordination. It relies on a set of explicit rules to direct power flows between PV, battery, and grid. When PV production exceeds load, the surplus is first directed to the battery, up to a limit of 10 kW; any additional surplus is exported to the grid. Conversely, if the load exceeds PV production, the battery supplies the energy required up to 10 kW, and the grid makes up the remainder of the deficit.

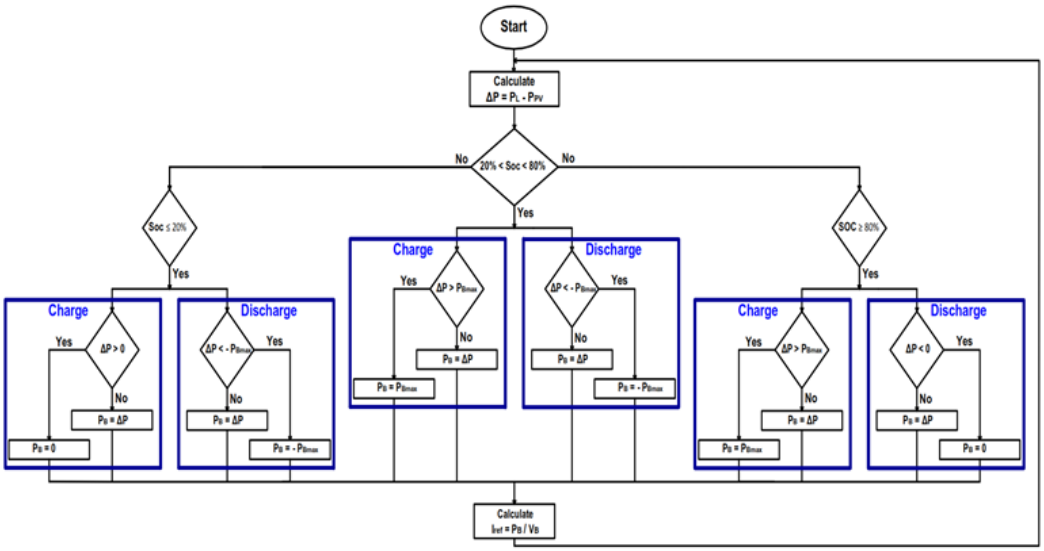

Fig.12. Flowchart of the proposed charging and discharging management strategy.

The EMS also manages critical situations: if the battery reaches its SOCmax, excess PV power

is exported directly to the grid; if it reaches its SOCmin, the grid takes over to supply the load. This approach guarantees robust, reliable energy management, optimizing self-consumption and microgrid stability. Fig.12 presents the operational scenarios governed by the proposed EMS algorithm.

The battery's charging and discharging power is controlled by regulating its current (IB). To do this, the algorithm calculates the reference current (Iref) based on the scenarios described above. Then, a PI controller ensures that the IB current precisely follows the Iref current in real-time. Fig.13 shows the MATLAB/Simulink implementation of this system.

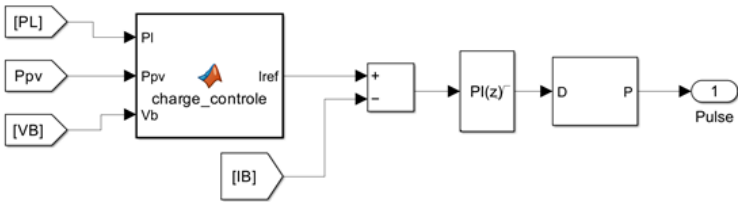

Fig.13. Simulink implementation of the charging/discharging control for the BESS.

3. RESULTS AND DISCUSSION

This section presents the detailed results of the simulations carried out to evaluate the performance of the proposed EMS for the hybrid microgrid. All simulations were achieved using the MATLAB/Simulink environment, where each block and component of the system was implemented and simulated as shown in Fig.14

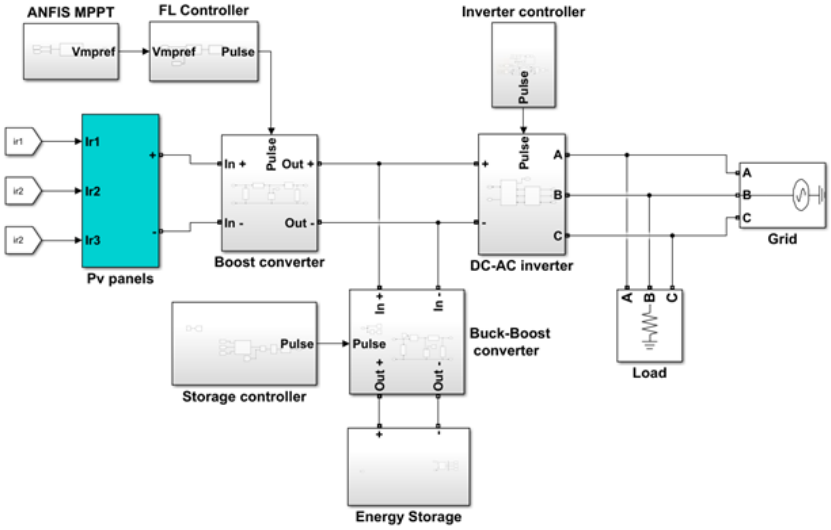

Fig.14. System implementation in Simulink.

The analysis of the results will focus on several key aspects. Firstly, we will evaluate the MPPT's performance under uniform and partial shading conditions. Secondly, we will examine the balance of power flows and the smooth operation of energy distribution between the battery and the grid. Finally, particular attention will be paid to critical case management and battery SOC behavior, to validate the reliability of the charge/discharge management algorithm.

Specifications for the various system components are calculated based on the methods presented in [8]. These are shown in Table 2.

To evaluate the robustness and efficiency of our system, various irradiance profiles were selected. These profiles include uniform and variable real-time shading conditions (the first 12 seconds), as well as partial shading scenarios (the last 6 seconds), in order to test the MPPT control's ability to

maximize the power extracted from the photovoltaic panels in all situations. The irradiance used is shown in Fig.15.

Table 2. System specifications.

PV (1000 W/m²)	Boost Converter	Buck-Boost Converter	Battery	Grid
Ppv max: 50 kW	Input capacitor: 100 µF	Input capacitor: 1 mF	Type: lithium-ion	Phase-to-phase Voltage (Vrms): 380 V Frequency: 50 Hz
Vpv max: 415 V	Output capacitor: 1 mF	Output capacitor: 10 µF	Capacity: 150 Ah	
Ipv max: 120.5 A	Inductance: 9.6575 mH	Inductance: 130 mH	Maximum power: 10 kW	

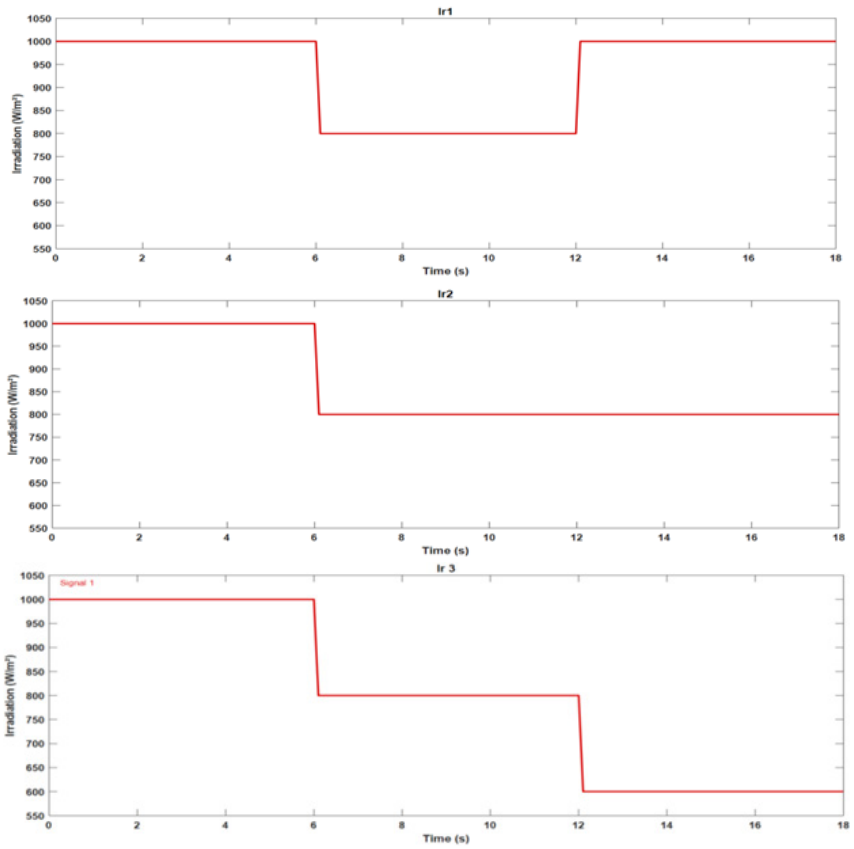

Fig.15. Irradiation profile used.

According to the panel characteristics shown in Fig.3 and Fig.4, under uniform irradiation conditions of 1000 W/m², the maximum expected power is around 50 kW. When irradiation is reduced to 800 W/m², the maximum expected power is around 40 kW. On the other hand, under conditions of partial shading, where each group of panels receives separate irradiation, the maximum total power supplied by the system is around 33 kW.

With regard to load, the system was subjected to two distinct levels of demand: a 35 kW load and a 55 kW load. These scenarios were analyzed by considering both normal (where the battery SOC is between 20% and 80%) and critical (where the SOC is less than or equal to 20% or greater than or equal to 80%) operating situations, enabling us to assess the behavior of the microgrid under various conditions.

3.1. First case (Load power demand of 35 KW)

3.1.1. First scenario (Normal SOC situation (20% < Soc <80%))

In this first scenario, a constant load demand of 35 kW was considered, with the batteries initially charged to 50%. Fig.16 shows the various power curves (PV production, load consumption, battery power, and exchanges with the grid), while Fig.17 illustrates the evolution of the battery's SOC.

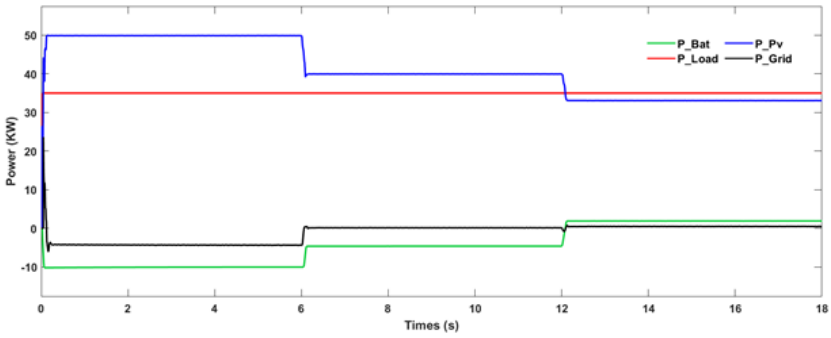

Fig.16. PV, load, battery, and grid power curves for a 35 kW load and normal SOC.

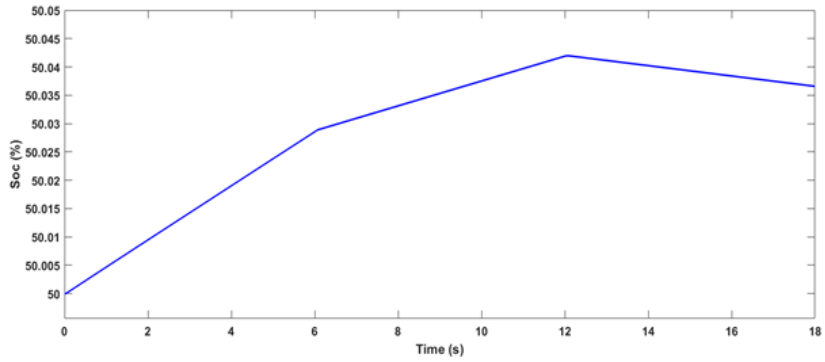

Fig.17. Battery SOC variation for a 35 kW load and normal SOC.

Evaluation of the ANFIS-FL MPPT control and battery management algorithm (Fig.16 and Fig.17) under uniform irradiance and partial shading:

- PV output varies between three levels:
  - 50 kW (0–6 s).
  - 40 kW (6–12 s).
  - 33 kW (12–18 s).
- Simulation results match theoretical expectations.
- The ANFIS-FL MPPT control shows high accuracy in tracking the maximum power point (MPP)

Power flow analysis (Fig.16):

- 0–6 s: PV produces 50 kW; load consumes 35 kW; 10 kW stored in battery; 5 kW exported to grid.
- 6–12 s: PV output = 40 kW; load = 35 kW; surplus of 5 kW fully stored in battery.
- 12–18 s: PV output = 33 kW; load = 35 kW; deficit of 2 kW fully supplied by the battery.
- These observations confirm the algorithm's ability to ensure accurate control of battery power. Respects the 10 kW maximum charge/discharge limit for safety. Maintains optimal energy balance between PV, battery, load, and grid.

Battery SOC evolution (Fig.17):

- 0–6 s: SOC increases from 50% to around 50.03% (10 kW charging limit applied).
- 6–12 s: SOC rises more slowly to around 50.042% (5 kW surplus fully absorbed).

- 12–18 s: SOC decreases slightly from around 50.042% to 50.037% (battery discharges 2 kW to cover the deficit).
- Confirms the algorithm's effectiveness in rule-based SOC management.

3.1.2. Second scenario (Critical SOC situation (80% ≤ Soc))

The batteries in this situation are assumed to be fully charged (SOC ≥ 80%) at around the 9th second, to assess the algorithm's ability to react.

Fig.18. PV, load, battery, and grid power curves during a high SOC scenario fo.

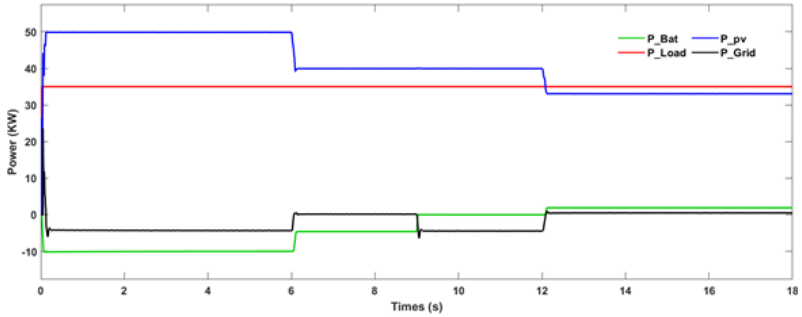

Fig.18. PV, load, battery, and grid power curves during a high SOC scenario for a 35 kW load.

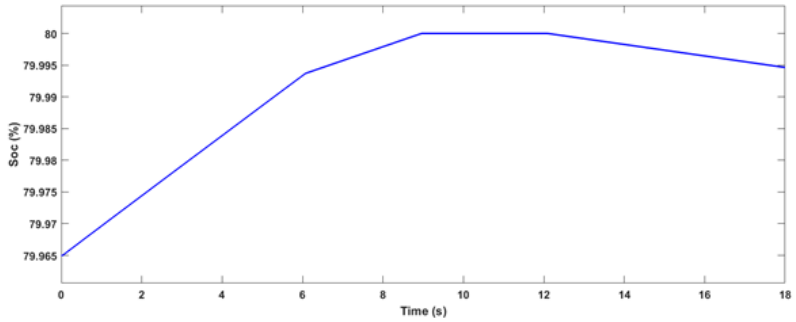

Fig.19. Battery SOC variation during a high SOC scenario for a 35 kW load.

As described in Scenario 1:

- When the battery SOC reaches SOCmax = 80% (Fig.18 and Fig.19), charging stops and all surplus PV power is exported to the grid.

In this case:

- SOC rises from 79.965% to 80% at around 9 seconds (triggers the high-SOC rule).
- PV power = 40 kW ; Load = 35 kW ; Surplus = 5 kW.

EMS response:

- Battery power drops to 0 kW (charging stops).
- Grid export increases to around 5 kW.

This confirms the algorithm's ability to detect and manage critical high-SOC conditions while preserving microgrid balance.

3.2. Second case (Load power demand of 55 KW)

3.2.1. First scenario (Normal Soc situation (20% < Soc < 80%))

In this scenario, a constant load demand of 55 kW was applied to assess the algorithm's ability to handle larger power deficits. The batteries are initially charged to 50%. Fig.20 shows the various power curves (PV production, load consumption, battery power, and exchanges with the grid), while Fig.21 illustrates the evolution of the battery's SOC.

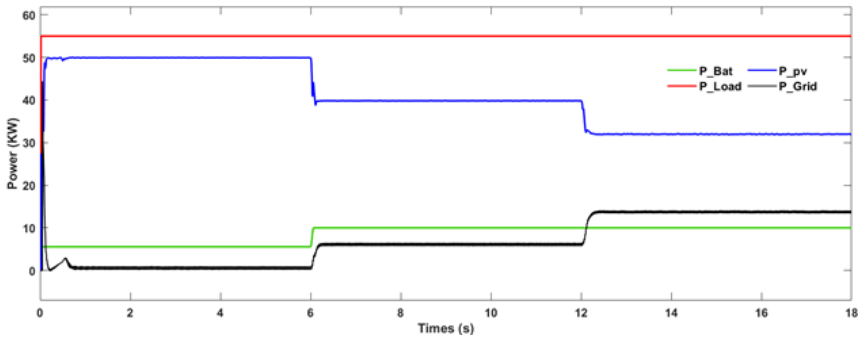

Fig.20. PV, load, battery, and grid power curves for a 55 kW load and normal SOC.

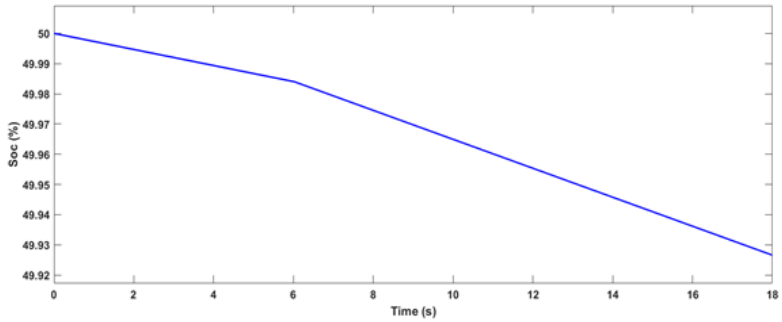

Fig.21. Battery SOC variation for a 55 kW load and normal SOC.

EMS prioritizes covering power deficits with the BESS (up to 10 kW) before drawing from the grid.

- 0–6 seconds (Fig. 20 & Fig. 21):
- PV output = 50 kW, load = 55 kW; deficit = 5 kW.
- BESS supplies 5 kW, grid inactive.
- SOC decreases slightly from 50% to 49.985%.
- 6–12 seconds:
- PV output = 40 kW, load = 55 kW; deficit = 15 kW.
- BESS provides 10 kW (limit).
- Grid supplies the remaining 5 kW.
- SOC decreases more rapidly.
- 12–18 seconds:
- PV output = 33 kW, load = 55 kW; deficit = 22 kW.
- BESS continues at 10 kW.
- Grid supplies the remaining 12 kW.

Power balance is maintained. Confirming the robustness of the EMS under sustained deficit conditions.

3.2.2. Second scenario (Critical Soc situation (Soc ≤ 20%))

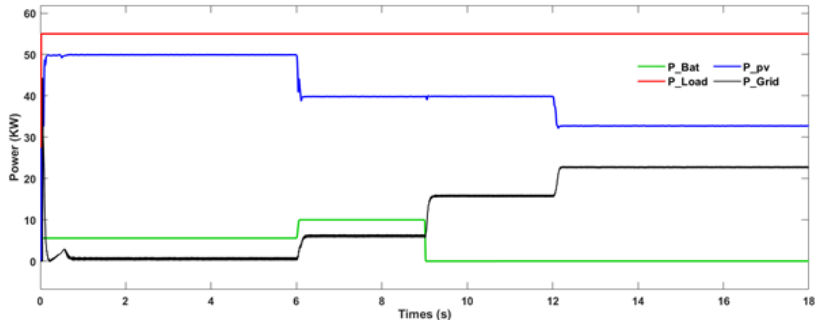

Fig.22. PV, load, battery, and grid power curves during a low SOC scenario for a 55 kW load.

In this situation, it is assumed that the batteries reach their minimum discharge limit (SOC ≤ 20 %) at around the 9th second, to assess the algorithm's ability to react.

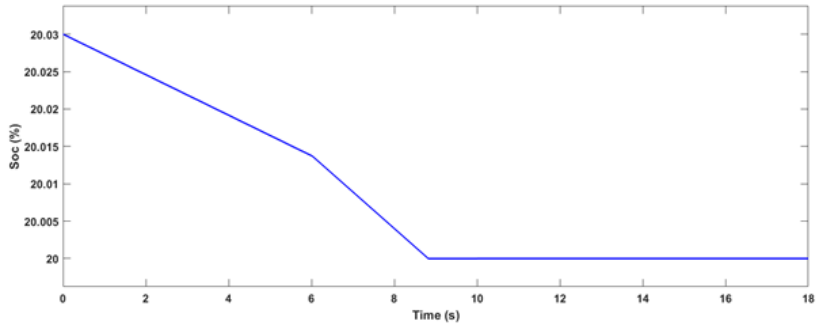

Fig.23. Battery SOC variation during a low SOC scenario for a 55 kW load.

Once SOC reaches SOCmin (20%), EMS stops discharging the BESS and shifts entirely to grid support.

At 9 seconds (Fig. 23):

- SOC decreases from 20.03% to 20%, then remains stable.
- At the same time (Fig. 22):
- PV output = 40 kW, load = 55 kW, deficit = 15 kW.
- Battery power decreases from –10 kW to 0 kW.
- Grid import rises to 15 kW, covering the entire deficit.

This confirms the EMS's ability to protect the battery and maintain supply continuity under critical low-SOC conditions.

3.3. Quantitative comparison with existing MPPT techniques

To provide a stronger contextual basis for this study, we refer to our previous research [12], which evaluated the performance of three MPPT techniques, P&O, PSO, and ANN combined with a fuzzy logic controller under both uniform irradiation and partial shading conditions. This comparison helps to highlight the strengths and weaknesses of each approach relative to the proposed ANFIS-based method. While a fully quantitative comparison would require identical system configurations and test conditions, we can still identify overall trends by analysing the performance characteristics observed in both studies.

Under uniform irradiation, all methods were generally effective at tracking the maximum power point. The P&O approach, however, showed significant oscillations around the MPP, which could compromise stability. The PSO technique successfully reached the MPP but needed longer convergence times due to the large number of iterations required. The ANN method with a fuzzy logic controller provided faster and more accurate tracking, though the additional controller introduced a slight delay, making its response comparable to the ANFIS-based method.

In partial shading scenarios, the P&O method struggled due to its tendency to settle on local maxima, limiting tracking accuracy. Both PSO and ANN with fuzzy logic performed well, with ANN exhibiting quicker response times, while PSO required more iterations to reach the optimal point.

4. CONCLUSION

This work presented a robust EMS for a microgrid integrating PV panels, a BESS, and a grid connection. The proposed EMS ensures dynamic and reliable power balance while maximizing solar self-consumption under operational constraints. An ANFIS–Fuzzy Logic MPPT controller was implemented and demonstrated high performance, achieving a maximum power capture

error of ±0.06 kW, a power-balance error below ±0.02 kW across all tested scenarios, and an overall system response time of 0.125 seconds.

A key contribution of this study lies in the rule-based battery management algorithm, which enforces a strict 10 kW charge/discharge limit. This constraint ensures safe and reliable operation of the BESS while accurately coordinating power flows among PV, battery, load, and grid, including the handling of critical SOC events (at SOCmin and SOCmax). Simulation results under defined irradiance and load profiles confirmed the accuracy, stability, and robustness of the proposed EMS.

Despite these promising results, some limitations remain. The system's auxiliary or self-consumption was not evaluated. Complex dynamic climate conditions, such as rapid irradiance ramps caused by moving clouds, seasonal variations, or combined temperature effects, were not modelled. Furthermore, the performance was validated only through simulations, without experimental testing on a physical prototype. These aspects could influence real-world behavior and will be addressed in future research.

Looking ahead, several directions can be explored to extend this work. One important improvement would be to replace the fixed 10 kW charge/discharge limit with a smart adaptive bound that depends on SOC, temperature, and PV/load conditions. Practical implementation on hardware, coupled with a detailed economic evaluation, will also be carried out. The integration of real-time forecasting for PV production and load demand, together with the consideration of complex dynamic climate conditions, will further enhance the system's reliability. In addition, extending the analysis to reactive power management, including the use of devices such as STATCOM, will improve voltage stability and power quality. Finally, the interconnection of multiple microgrids will be studied to enable mutual energy exchanges, strengthen resilience, and optimize the use of renewable resources.

Author Contributions: All authors have made a substantial, direct, and intellectual contribution to the work and approved it for publication.

Funding: This article received no external funding.

Data Availability Statement: All the data are available in the manuscript.

Acknowledgments: The authors gratefully acknowledge the support provided by the Engineering and Applied Physics Team (EAPT) at the Higher School of Technology, Sultan Moulay Slimane University, Beni Mellal, Morocco. The authors also sincerely appreciate the editor and reviewers for their timely observations and suggestions regarding this research article.

Conflicts of Interest: The authors declare that they have no conflict of interest.

REFERENCES

[1].A. Giedraityte, S. Rimkevicius, M. Marciukaitis, V. Radziukynas, and R. Bakas, "Hybrid renewable energy systems—A review of optimization approaches and future challenges," Applied Sciences, vol. 15, no. 4, p. 1744, 2025, https://doi.org/10.3390/app15041744

[2].M. Ahmad, M. Shafiullah, C. B. Ahmed, and M. Alowaifeer, "A review of microgrid energy management and control strategies," IEEE Access, vol. 11, pp. 21729–21757, 2023, https://doi. org/10 .1109/ACCESS.2023.3248511

[3].B. Lei, Y. Ren, H. Luan, R. Dong, X. Wang, J. Liao, S. Fang, and K. Gao, "A review of optimization for system reliability of microgrid," Mathematics, vol. 11, no. 4, p. 822, 2023, https:// doi. org/10.3390/math11040822

[4].H. J. C. Conde, C. M. Demition, and J. Honra, "Storage is the new black: A review of energy storage system applications to resolve intermittency in renewable energy systems," Energies, vol. 18, no. 2, p. 354, 2025, https://doi.org/10.3390/en18020354

[5].A. W. Adegboyega, S. Sepasi, H. O. R. Howlader, B. Griswold, M. Matsuura, and L. R. Roose, "DC microgrid deployments and challenges: A comprehensive review of academic and corporate implementations," Energies, vol. 18, no. 5, p. 1064, 2025, https://doi.org/10.3390/en18051064

[6].C. Ghizlane, M. Boulouiz, A. Boulouiz, and A. Abdelouahed, "Performance analysis of MPPT tracking algorithm based on artificial neural network for a PV pumping system," in Proc. 4th Int. Conf. Innovative Research in Applied Science, Engineering and Technology (IRASET), Fez, Morocco, 2024, pp. 1–7, https://doi.org/10.1109/IRASET60544.2024.10548482.

[7].M. A. Atillah, H. Stitou, A. Boudaoud, and M. Aqil, "Performance analysis of three MPPT controls under partial shading: P&O, PSO and ANN," E3S Web of Conferences, vol. 469, p. 00064, 2023, https://doi.org/10.1051/e3sconf/202346900064.

[8].M. A. Atillah, H. Stitou, A. Boudaoud, and M. Aqil, "Comparative study of two ANFIS-based MPPT controls under uniform and partial shading conditions," Solar Energy and Sustainable Development Journal, vol. 14, no. SI_MSMS2E, pp. 89–103, 2024, https://doi.org/10.51646/jsesd.v14iSI_MSMS2E.400

[9].S. Siddaraj, U. R. Yaragatti, and N. Harischandrappa, "Coordinated PSO-ANFIS-based 2 MPPT control of microgrid with solar photovoltaic and battery energy storage system," Journal of Sensor and Actuator Networks, vol. 12, no. 3, p. 45, 2023, https://doi.org/10.3390/jsan12030045

[10]. E. Kalaiyarasan and S. Singaravelu, "Efficient power management system of PV, fuel cell and BESS-based DC microgrid system," International Journal of Recent Engineering Science, vol. 11, no. 4, pp. 81–92, 2024, https://doi.org/10.14445/23497157/IJRES-V11I4P111

[11]. V. Dhanunjaya, B. Ausali, and N. K. Golla, "Hybrid energy management-based intelligent ANFIS control for smart DC-microgrid," in Recent Evolutions in Energy, Drives and e-Vehicles, REEDEV 2022, N. K. Dhote, M. L. Kolhe, and M. Rehman, Eds. Singapore: Springer, Lecture Notes in Electrical Engineering, vol. 1162, 2024, https://doi.org/10.1007/978-981-97-0763-8_29

[12]. M. A. Atillah, H. Stitou, A. Boudaoud, M. Aqil, and A. Hanafi, "Study and analysis of partial shading effect on power production of a photovoltaic string controlled by three different MPPT techniques: P&O, PSO and ANN," Mathematical Modeling and Computing, vol. 11, no. 3, pp. 856–869, 2024, https://doi.org/10.23939/mmc2024.03.856.

[13]. Y. Zhang and Y. Zhang, "An advanced digital predictive valley current control algorithm for a boost converter," Journal of Physics: Conference Series, vol. 1207, 3rd Int. Conf. Control Engineering and Artificial Intelligence (CCEAI 2019), Los Angeles, USA, Jan. 24–26, 2019, p. 012001, 2019, https://doi.org/10.1088/1742-6596/1207/1/012001

[14]. S. Chapala, R. L. Narasimham, and G. Tulasi Ram Das, "Power quality analysis of ANFIS based distributed generation system with UPQC," International Journal of Engineering and Manufacturing (IJEM), vol. 14, no. 4, pp. 1–14, 2024, https://doi.org/10.5815/ijem.2024.04.01.

[15]. A. N. Mohammed, S. Umar, and S. Chatterjee, "ANFIS systematic robustness investigation for AVR system," e-Prime - Advances in Electrical Engineering, Electronics and Energy, vol. 9, p. 100670, 2024, https://doi.org/10.1016/j.prime.2024.100670.

[16]. H. Stitou, M. A. Atillah, A. Boudaoud, and M. Aqil, "Load forecasting using fuzzy logic, artificial neural network, and adaptive neuro-fuzzy inference system approaches: application to South-Western Morocco," International Journal of Electrical & Computer Engineering, vol. 14, no. 6, 2024, http://doi.org/10.11591/ijece.v14i6.pp7067-7079.

[17]. L. Farah, A. Haddouche, and A. Haddouche, "Comparison between proposed fuzzy logic and ANFIS for MPPT control for photovoltaic system," International Journal of Power Electronics and Drive Systems, vol. 11, no. 2, p. 1065, 2020, http://doi.org/10.11591/ijpeds.v11.i2.pp1065-1073.

[18]. A. Dabiriaghdam, N. Jafarnia Dabanloo, F. N. Rahatabad, et al., "Design and stability analysis of an adaptive neuro-fuzzy inference system (ANFIS) based pacemaker controller in MATLAB Simulink," Preprint, Research Square, Apr. 5, 2023, https://doi.org/10.21203/rs.3.rs-2753442/v1

[19]. J. Lorenzo, J. C. Espiritu, J. Mediavillo, S. J. Dy, and R. B. Caldo, "Development and implementation of fuzzy logic using microcontroller for the buck and boost DC-to-DC converter," in IOP Conference Series: Earth and Environmental Science, vol. 69, no. 1, p. 012193. IOP Publishing, 2017, http://doi.org/10.1088/1755-1315/69/1/012193.

[20]. H. Stitou, M. A. Atillah, A. Boudaoud, and M. Aqil, "Medium-term load forecasting using the fuzzy logic approach: A case study of Taroudannt province," in E3S Web of Conferences, vol. 469, p. 00063. EDP Sciences, 2023, https://doi.org/10.1051/e3sconf/202346900063.

[21]. L. F. Grisales-Noreña, C. A. Ramos-Paja, D. Gonzalez-Montoya, G. Alcalá, and Q. Hernandez-Escobedo, "Energy management in PV based microgrids designed for the Universidad Nacional de Colombia," Sustainability, vol. 12, no. 3, p. 1219, 2020, https://doi.org/10.3390/su12031219

[22]. M. A. Atillah, H. Stitou, A. Boudaoud, and M. Aqil, "Power Flow Management for Off-Grid Photovoltaic-Battery System Using ANN-FL Controller MPPT," International Conference on Connected Objects and Artificial Intelligence, pp. 158-164. Cham: Springer Nature Switzerland, 2024, https://doi.org/10.1007/978-3-031-70411-6_25.

[23]. J. Wang, B. Wang, L. Zhang, J. Wang, N. I. Shchurov, and B. V. Malozyomov, "Review of bidirectional DC–DC converter topologies for hybrid energy storage system of new energy vehicles," Green Energy and Intelligent Transportation, vol. 1, no. 2, p. 100010, 2022, https://doi.org/10.1016/j.geits.2022.100010.